Researchers Journal of Science and Technology (REJOST)
https://rejost.com.ng

Electrical resistivity gradients as valuable tools for the parameterization of subterranean heterogeneity and aquifer vulnerability to contamination

Otobong S. Ukpe, * Ndifreke I. Udosen, Jewel E. Thomas

Received: July 17, 2024 /Accepted: September 23, 2024

Abstract

This work demonstrates that electrical resistivity gradients are valuable for the characterization of subsurface heterogeneity and aquifer vulnerability to contamination. Field data was obtained via geo-electrostratigraphic techniques integrated with ground truth information from lithological boreholes. Vertical electrical soundings were undertaken along 19 profile lines and electrical resistivity tomography surveys were undertaken along 4 profile lines. The resistivity curves generated by WINRESIST described four geo-electrostratigraphic layers. The uppermost stratum (motley/heterogeneous topsoil) had resistivity measures of 95.2 - 1463.7 Ωm with a 0.6 - 6.6 m thickness. The second lithological layer (clayey sand) had resistivity values of 8.8 - 2485.1 Ωm with a thickness of 2.3-114.6 m. The third lithological stratum (fine/medium-grained sands) had resistivity values ranging from 72.5- 1332.7 Ωm with a thickness of 34.9 – 123.7 m. The fourth lithological stratum had resistivity measures of 82.0- 1808.6 Ωm. Mean values of electrical resistivity gradients for layers 1 and 2 were 411.42Ω and 53.22Ω, respectively. Iso-parametric maps of longitudinal conductance and electrical resistivity gradient (longitudinal resistance) indicated that the majority of the investigation area had weak aquifer protectivity. The transverse resistance, with a gamut of 3669.93 – 79868.18Ωm^2 and a mean value of 20451.34 Ωm^2, indicated that the region had prolific groundwater potential. The electrical resistivity gradient measures were integrated with measures of the electrical reflection coefficient, the goal being to investigate the degree of subsurface heterogeneity. The regression curves of the electrical reflection coefficients were 90^o out of phase, indicating alternating beddings of diverse lithological facies. Utilization of electrical resistivity gradient and electrical reflection co-efficient measures generated information on subsurface heterogeneity with depth and

aquifer vulnerability to contamination. This work has illustrated that measures of electrical resistivity gradient are valuable for parameterizing subterranean variability and groundwater susceptibility to toxicants.

✉ Ndifreke Udosen: *ndifrekeudosen@aksu.edu.ng*, *ndifreke.udosen@yahoo.com*

Department of Physics (Geophysics Research Group), Akwa Ibom State University, Nigeria

Keywords: Aquifer vulnerability; longitudinal resistance; longitudinal conductance; reflection coefficient; electrical resistivity

1.0 Introduction

The sustainability and availability of potable groundwater resources is critical for the establishment of effective subterranean water management practices (Choudhury *et al*., 2001; Sikandar and Christen, 2012; Ekwe and Opara, 2012; Suneetha and Gupta, 2018; Ekwe *et al*., 2020; Ibuot *et al*., 2021; Ishak *et al*., 2022; George *et al*., 2022; Mohammed *et al*., 2023a, b; Udosen *et al*., 2024a, b; George *et al*., 2024; Vijayaprabhu *et al*., 2024; Zaini and Hasan, 2024). Via geophysical investigations, one may generate valuable information on the potentiality of aquifer reserves within a region (Yadav and Abolfazli, 1998; Srinivasa Gowd, 2004; Kenneth and Ebifuro, 2012; Aizebeokhai and Oyebanjo, 2013; Ugada *et al*., 2014; Eke *et al., 2015;* Sathiyamoorthy and Ganesan, 2018; Udosen and George, 2018a; Ejiogu *et al*., 2019; Warsi *et al*., 2019; George, 2020; Ebong *et al*., 2023). Geophysical investigations also aid in determining the degree of subsurface contamination arising from the leaching of waste material into the aquifer reserves (Udosen *et al*., 2022; Zaini and Hasan, 2024; Udosen *et al*., 2024c, d; Dauda and Ali, 2024). Assessing groundwater protective capacity requires proper investigation of the motion of toxicants via the vadose zone (Edet, 2004; Chandra *et al*., 2008; Atakpo and Ayolabi, 2009; Adeniji *et al*., 2014; George *et al*., 2017; Inim *et al*., 2020; Asfahani, 2023a, b; Sankar *et al*., 2023; Ekanem and Udosen, 2023a, b; Udosen *et al*., 2024e; Akiang *et al*., 2024; Olorunfemi *et al*., 2024). This assessment involves generating information on the porousness and permeability of the groundmass of the rock overlying the aquifer (George *et al*., 2018, Udosen 2024f, g). Regions having argillaceous sedimentary formations are more likely to encounter reduced permeabilities that preclude contaminant percolation and offer protectivity to subterranean water resources (Udosen *et al*., 2024h). Reduced aquifer protectivity, on the other hand, is more likely to occur in formations with open pore spaces and large fractures. For subterranean water resources to be guarded from contamination, geophysical investigations are critical.

Groundwater potentiality measures the quantity and quality of subsurface water that may be abstracted from water reservoirs without causing adverse damage to the aquifer overburden (Batte et al., 2010; Obiora et al., 2015, 2016; Eyankware *et al*., 2020; Eyankware and Aleke, 2021; Ibuot and Obiora, 2021). Although surface water resources abound in most coastal milieus, their accessibility and dependability are at times restricted. Groundwater resources are more crucial in such locations more crucial in such locations for satisfying the domestic and industrial needs of the populace. An increase in water demand puts an enormous strain on groundwater supplies in locations where groundwater is the predominant potable water source. The investigation site in this work, for example, is heavily dependent on subterranean water resources. The water resources

are under pressure due to a burgeoning population and the associated industrialization. Although some surface water sources like streams and lakes exist, they are highly vulnerable to pollution. In addition, the existing surface water sources experience seasonal changes, reducing their availability during arid periods. This makes subterranean water resources paramount for potability and maintaining diverse economic activities. Numerous obstacles may nevertheless preclude groundwater resources in the area from being sustainable. The aquifer system may be contaminated via inappropriate waste disposal and other anthropogenic activities that endanger groundwater quality, making the water resource unfit for human consumption (Aweto, 2011; Arowoogun and Osinowo, 2022; Okoroh and Ibuot, 2022; Inyang *et al*., 2024; Ojo *et al*., 2024). Once a water reservoir is employed as a potable water resource, effective management becomes critical to ensure non-deterioration of water quality (Ndatuwong and Yadav, 2015; Oni *et al*., 2017; Oloruntola *et al*., 2017; Agbasi *et al*., 2019; Nisar *et al*., 2021).

Electrical resistivity gradient, otherwise termed longitudinal resistance, was employed in this work for the parameterization of subsurface heterogeneity and aquifer vulnerability to contamination. The resistivity gradient is a second-order geoelectrical parameter generated from measures of first-order geo-electrical indices, which include the strata resistivity, thickness, and depth (Onuoha and Mbazi, 1988; Rai *et al*., 2013; Udosen and George, 2018b, George, 2021; Opara *et al*., 2023). The resistivity gradient is the inverse of longitudinal conductance (Ω^{-1}), a key Dar-Zarrouk parameter employed in assessing groundwater protectivity (Oladapo *et al*., 2004; Braga and Francisco, 2014; Naidu et al., 2021; Sirsat *et al*., 2023). Electrical resistivity gradient is defined as the ratio of geo-layer resistivity to the geo-layer unit thickness). Electrical resistivity gradients give information on subsurface heterogeneity and the ease with which the overburden can be penetrated by contaminants.

Several methodologies have been employed to evaluate subterranean water contamination resulting from pollutants percolating into geological units. Each methodology has its advantages and disadvantages, with no methodology being competent in all geological climes. Some of these methodologies employ index-based aquifer vulnerability models like the GOD model, the GALDIT model, the Aquifer Vulnerability Index (AVI) model, the SINTAC model, and the DRASTIC model, among others (Foster, 1987; Stempvoort *et al*., 1993; Civita, 1994; Lobo-Ferreira *et al*., 2007; Saha and Alam, 2014; Adebiyi *et al*., 2019; Udosen *et al*., 2023; Udosen *et al*. 2024i; Jamaa *et al*., 2024; Baki *et al*., 2024; Mohan *et al*., 2024; Mehta *et al*., 2024; Ourarhi *et al*., 2024). The above models, though effective, do generate somewhat subjective results since some of the parameters employed are not obtained via quantitative interpretation.

The aim of this work was the utilization of electrical resistivity gradient measurements, coupled with other key second-order geoelectrical parameters, in the parameterization of subsurface heterogeneity and aquifer vulnerability to pollution. This methodology will generate more accurate results, given that the parameters employed will be obtained via quantitative computations. Via subdividing the geologic column into units having predefined resistivity measures and geo-layer thickness through which current can permeate, resistivity gradient models, integrated with models of longitudinal conductance and electrical reflection coefficient will be generated that would give information on the subterranean resistivity variability and aquifer protectivity. Electrical resistivity gradient, longitudinal conductance, and electrical reflection co-efficient measures vary according to the geo-

electrical characterization of the investigated region, consequently, key geological information generated from these measures are critical in the characterization of lithological heterogeneity and the assessment of groundwater vulnerability to contamination.

2.0 Geology

The survey area is situated in Mkpat Enin, western Akwa Ibom State, southern Nigeria (Figures 1a and b). The region exists in an alluvial environment, has an approximate area of 400 km^2, and lies between latitudes 4°30′ - 4°35′ N and longitudes 7º30′ - 7º35′ E. The region's climate is a subtropical climate with discrete seasons: dry and rainy. The dry season starts in October and terminates in March whereas the rainy season starts in April and terminates in September. Temperatures during the dry season range from 25- 35ºC, and annual rainfall within the region ranges from 200 to 320 cm.

Three litho-stratigraphic formations exist in the region with the oldest being the Shaly Akata Formation having Eocene to Recent age (Short and Stauble, 1967). The Akata Formation serves as the hydrocarbon reservoir rock for the region (Avbovbo, 1978; Petters *et al.,* 1989; Stacher, 1995) and intrudes into the younger overlying Agbada Formation. Shale swells, ridge sands, and other diapiric features intruding into the Agbada Formation are over-pressurized in the Akata Formation shales. The Agbada Formation (approximately 4km in thickness) serves as the primary reservoir rock for crude oil depositories across the Niger Delta. The Agbada Formation comprises sands, shales, and silts arranged in alternating sequences, within a fluvial environment. Overlying the Agbada Formation is the Benin Formation, whose litho-stratigraphic units comprise arenites intercalated with argillitic materials (Short and Stauble, 1967; Reijers and Petters, 1987). The Benin Formation, which is the youngest formation within the investigation area, serves as the main zone from which groundwater resources are abstracted.

3.0 Materials and Methods

Geo-electrical prospecting methodologies were utilized for the investigation. In the electrical resistivity method, the passage of current via geo-layers is analogous to current flow via conductors. Each subsurface geo-layer automatically served as a resistor to current flow based on the initial resistivity of that given geo-layer. From measures of resistance generated from the field resistivity meter, one could evaluate the apparent resistivity based on the electrode configuration employed. The VES interpretations were constrained with borehole lithological logs information (Thomas *et al*., 2020) generated close to the investigation area. To generate electrical sounding results consistent with lithostratigraphic information, 19 VES profile lines were investigated close to borehole information. Via employment of an Integrated Geophysical Instrument Service (IGIS) resistivity meter and its accompanying accessories, resistivity information was obtained with Schlumberger electrode configuration. The Schlumberger configuration employed dual current conductors A and B to insert electric current I directly into the basement, and dual potential conductors M and N, to appraise the corresponding potential differences V. The proportion of V to I generated measures of apparent resistance R_a such that

$$R_a = \frac{V}{I} \qquad (1)$$

Standard deviation values of less than 10% (as indicated on the liquid crystal display (LCD) of the resistivity meter) indicated accurate measures of apparent resistance. The MN/2 had a gamut of 0.25 – 30m, and AB/2 had a gamut of 1 – 150m. By altering the spread separating the potential electrodes, one could increase the strength of current injected into the subsurface.

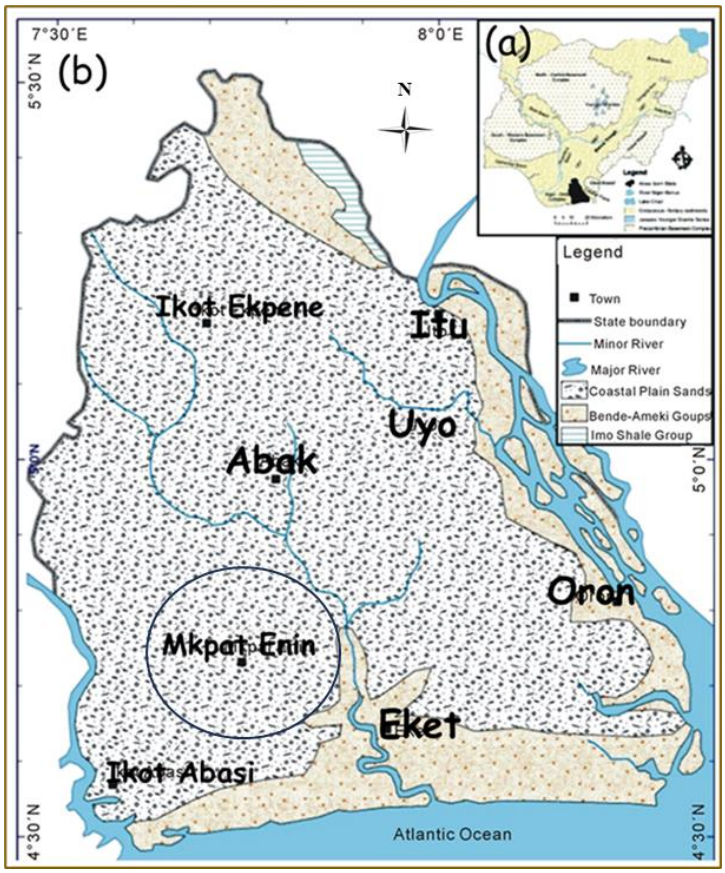

Figure 1a: Map of the region under investigation. The study area is the encircled region (Adapted from Emmanuel, 2013).

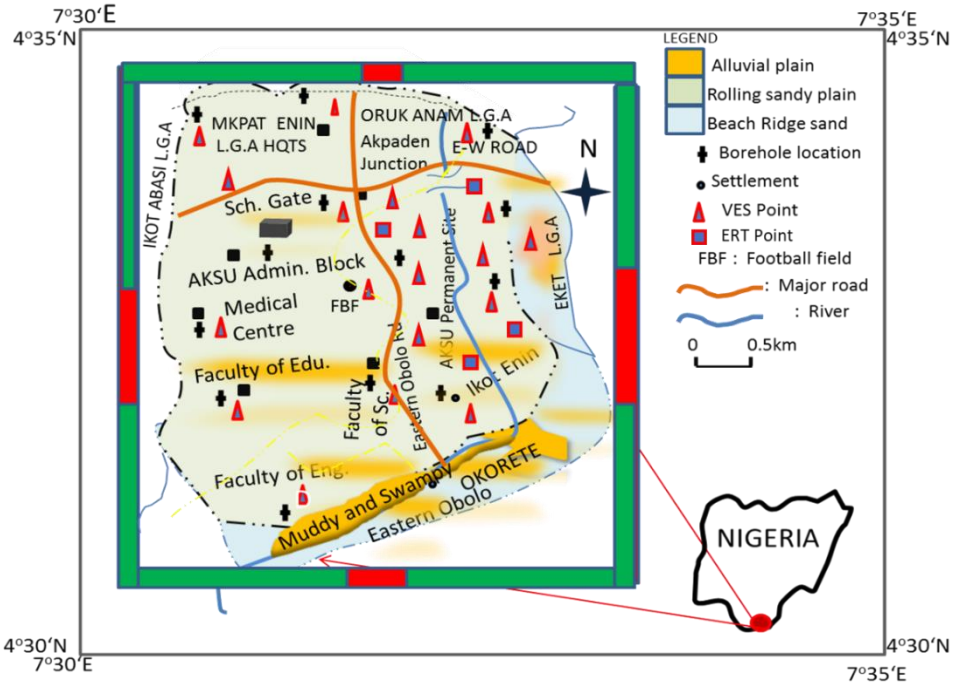

Figure 1b: Map showing the location of VES and ERT sample points (Adapted from Thomas et al. (2020))

The geometric factor G for the Schlumberger array is defined as

$$G = \pi \times \left\{ \frac{\left(\frac{AB}{2}\right)^2 - \left(\frac{MN}{2}\right)^2}{MN} \right\} \quad (2)$$

The measure for geometric factor G is reliant on the array type; G varies from one array type to another. The value of geometric factor G as described by equation (2) was multiplied by the value of apparent resistance R_a obtained from the Liquid Crystal Display (LCD) screen of the resistivity meter to generate measures of apparent resistivity ρ_a as follows:

$$\rho_a = GR_a \quad (3)$$

The apparent resistivity field data was converted to its corresponding geologic models via the employment of the WINRESIST software (Vander Velpen and Sporry, 1993).

Measurements were considered accurate when the root mean square (RMS) error was < 10%, indicating a small variance between field and theoretical data. Geological images obtained from vertical electrical soundings indicated the resistivity, thickness, and depth of the litho-stratigraphic layers (Zohdy, 1974; Vander-Velpen, 1988; Loke *et al*., 2001; Loke and Dahlin, 2002; Samouëlian *et al*., 2005; Frifita *et al*., 2024; Alao *et al*., 2024).

In addition to the employment of vertical electrical soundings in the delineation of the first-order geo-electrical parameters, four electrical resistivity tomography (ERT) profile lines were investigated. The essence of undertaking the ERT surveys alongside the vertical electrical soundings (VES) was to generate high-resolution 2D images that would delineate the lateral and vertical variation in the geo-electrostratigraphic information. The tomographic images obtained from ERT would serve to complement results obtained from VES, and the integration of the information from the two geophysical techniques would give more comprehensive information than would be obtained from the employment of one technique alone. A Wenner array configuration was employed for the ERT survey. The array had a minimum electrode spacing of 5m and a maximum electrode spacing of 105m, and the electrodes were placed at equal distances from each other. The current electrodes (AB) were used to insert current, and the potential electrodes (MN) measured the potential difference generated between the current electrodes. The geometric factor G for the Wenner configuration is defined as:

$$G = 2\pi a \quad (4)$$

with the parameter a being the equidistant interval between the electrodes. This geometric factor G was multiplied by the values of apparent resistance R_a to produce estimates of apparent resistivity ρ_a such that:

$$\rho_a = GR_a \quad (5)$$

Conversion of the apparent resistivity information into geologic models was via the reconstruction algorithm RES2DINV (Loke and Barker, 1996; Loke *et al*., 2001; Loke and Dahlin, 2002). The problem of resistivity imaging is ill-posed (Groetsch and Groetsch, 1993; Engl *et al*., 1996; Zhdanov, 2002; Udosen *et al*., 2011; 2013a, b; Udosen and Potthast, 2018; 2019; Richter, 2021; Bertero *et al*., 2021), hence it required regularization schemes to generate stable solutions. The geologic models generated from the RES2DINV reconstruction algorithm were considered accurate when the root mean square (RMS) error on the tomograms was < 10%. Such reduced values of RMS errors indicated minimal variation between the field information and the computed data. The tomographic images delineated the perpendicular and lateral diversity of subterranean resistivity across the profile lines. Precautions were carried out to enable the acquisition of

accurate data that represented the true litho-stratigraphic profile of the survey area. These precautions included the avoidance of locations of underground pipes, electrical power lines, and other electromagnetic radiations, the goal being to preclude the inclusion of anomalous information that did not represent the true subsurface information. Another precaution was the check to ensure adequate ground-electrode contact, the goal being to ensure that current injected via the resistivity meter permeated the earth's surface. Other precautions were the establishment of an equivalent of an equivalent distance spread for the conductors, and the avoidance of built-up locations when determining where to situate profile lines.

The first-order geoelectrical indices were employed in the computation of the resistivity gradients that would enable the evaluation of the subsurface heterogeneity and the water reservoir's susceptibility to toxicants. The resistivity gradient is the inverse of longitudinal conductance S_L, a key Dar-Zarrouk parameter. Longitudinal conductance S_L is given by:

$$S_L = \sum_i^n \frac{h_i}{\rho_i} \qquad (6)$$

with h as thickness of subterranean layers overlying the aquifer, and ρ as resistivity of subterranean layers overlying the aquifer. The second Dar-Zarrouk parameter, transverse resistance, was also evaluated to indicate aquifer potentiality within the region. Transverse resistance T_R measures were obtained via the empirical formulation:

$$T_R = \sum_i^n h_i \rho_i \qquad (7)$$

The electrical resistivity gradient (RG) was evaluated via:

$$RG = \sum_i^n \frac{1}{S_{L_i}} \qquad (8)$$

to give

$$RG = \sum_i^n \frac{\rho_i}{h_i} \qquad (9)$$

with h as thickness of subterranean layers overlying the aquifer and ρ as resistivity of subterranean layers overlying the aquifer. The measures of resistivity gradient were later employed to delineate how resistivity varied within each subsurface geo-layer. Each subsurface geo-layer has specified measures of resistivity gradient, which gives information on the nature of resistivity ρ_i for a given unit thickness h_i. Resistivity gradient (RG) would also be used to delineate quantitatively, the vulnerability of the aquifer to contamination.

To further assess how subsurface resistivity varied within the study area, reflection coefficient measures were employed. The reflection coefficient delineating the resistivity variation between the first and second litho-stratigraphic layers was given as:

$$k_{12} = \frac{\rho_2 - \rho_1}{\rho_2 + \rho_1} \qquad (10)$$

where k_{12} = reflection coefficient between first and second litho-stratigraphic layers, ρ_1= sub-surface resistivity of the first stratum, and ρ_2 = subsurface resistivity of the second stratum. The reflection coefficient describing the resistivity variation between the second and third layers was given as:

$$k_{23} = \frac{\rho_3 - \rho_2}{\rho_3 + \rho_2} \qquad (11)$$

where k_{23} = reflection coefficient between second and third litho-stratigraphic layers, ρ_2= subsurface resistivity of the second stratum, and ρ_3 = subsurface resistivity of the third stratum.

4.0 Results and Discussion

The resistivity curves generated by WINRESIST described four geo-stratigraphic layers (Table 1). The uppermost stratum (motley/heterogeneous topsoil) had resistivity measures of 95.2 - 1463.7 Ωm with a 0.6 - 6.6 m thickness. The second lithological layer (clayey sand) had resistivity values of 8.8 - 2485.1 Ωm with a thickness of 2.3-114.6 m.

Table 1: Summary of first-order geo-electrical parameters. The table illustrates that the thickness of lithological layers increased with subsurface depth

VES No.	Longitude	Latitude	No of strata	Stratum resistivity (Ωm)				Stratum thickness (m)			Stratum depth (m)			Curve type
				ρ1	ρ2	ρ3	ρ4	h1	h2	h3	d1	d2	d3	
1	7.778767	4.619278	4	632.40	189.30	1332.70	658.90	1.50	11.70	93.20	1.50	13.30	106.50	HK
2	7.77778	4.618333	4	514.40	1315.80	508.90	278.10	1.00	3.50	123.70	1.00	4.50	128.20	KQ
3	7.775753	4.620972	4	324.50	106.50	439.30	102.20	0.70	5.50	38.30	0.70	6.20	44.60	HK
4	7.778417	4.620472	4	403.40	110.40	574.90	258.00	6.60	6.50	78.40	6.60	13.10	91.50	HK
5	7.775583	4.623389	3	541.90	2116.70	300.00	-	3.30	33.00	-	3.30	36.30	-	K
6	7.771917	4.621278	4	344.30	50.50	583.20	87.60	1.70	18.10	53.30	1.70	19.70	73.00	HK
7	7.769833	4.621444	3	1319.80	514.20	283.80	-	1.40	114.60	-	1.40	116.00	-	Q
8	7.774972	4.620083	3	842.00	2485.10	376.40	-	1.00	31.80	-	1.00	32.80	-	K
9	7.776528	4.618306	4	249.90	55.80	506.40	82.00	1.80	11.20	34.90	1.80	13.10	48.00	HK
10	7.776234	4.618812	4	395.70	1567.10	510.30	1808.60	0.60	7.90	49.30	0.60	8.50	57.80	KH
11	7.7778251	4.624232	4	401.60	1108.40	481.90	1195.90	1.10	27.50	50.50	1.10	28.60	79.10	KH
12	7.762542	4.625431	3	563.40	966.10	1115.90	-	1.10	75.10	-	1.10	76.20	-	AK
13	7.764312	4.620323	4	183.10	21.40	640.20	117.10	0.90	2.30	51.40	0.90	3.20	54.60	AK
14	7.764213	4.621554	4	136.00	10.10	1236.30	289.10	2.00	5.90	76.80	2.00	7.90	84.70	HK
15	7.765765	4.623312	4	95.20	8.80	746.00	217.80	1.50	7.90	58.10	1.50	9.40	67.50	HK
16	7.755764	4.625323	4	1128.00	626.20	248.60	660.40	1.90	23.10	46.90	1.90	25.00	71.80	QH
17	7.756651	4.626434	4	268.40	1096.30	170.60	1433.50	1.50	15.80	45.70	1.50	17.30	63.00	KA
18	7.762621	4.618544	4	1463.70	88.80	86.50	429.00	1.30	19.90	56.50	1.30	21.20	77.70	QH
19	7.762586	4.616121	4	858.20	1069.20	72.50	271.50	2.90	16.80	63.00	2.90	19.70	82.80	KH

The third lithological stratum (fine/medium-grained sands) had resistivity values ranging from 72.5 - 1332.7 Ωm with a thickness of 34.9 - 123.7 m. The fourth lithological stratum had resistivity measures of 82.0- 1808.6 Ωm. The data indicated that the aquifer was located within the second and third lithological strata. Figure 2 illustrates borehole lithological data (Thomas et al., 2020) employed to constrain the vertical electrical soundings. Figures 3(a-c) depict maps illustrating the electrical resistivity variation of the first three geo-electrical layers. Different curve types were generated from the VES measures (Figure 4). From the measures of first-order geo-electrical indices delineated in Table 1, the second-order geoelectrical indices were computed (Table 2).

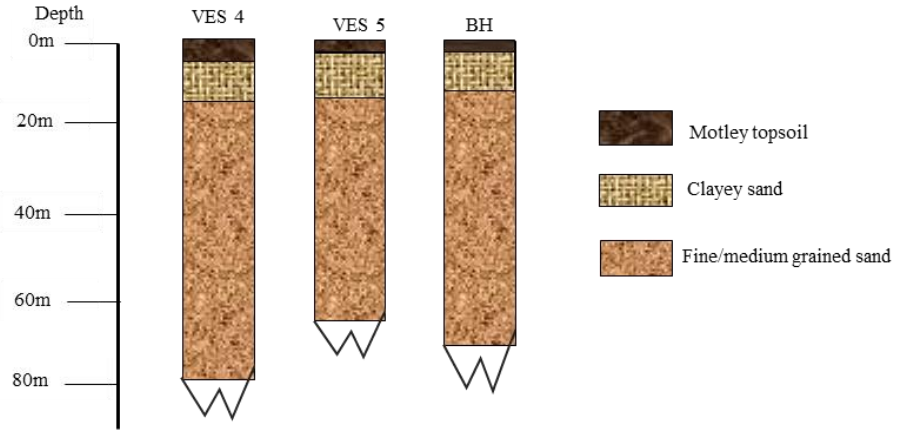

Figure 2: Borehole (BH) information correlated to vertical electrical sounding (VES) data

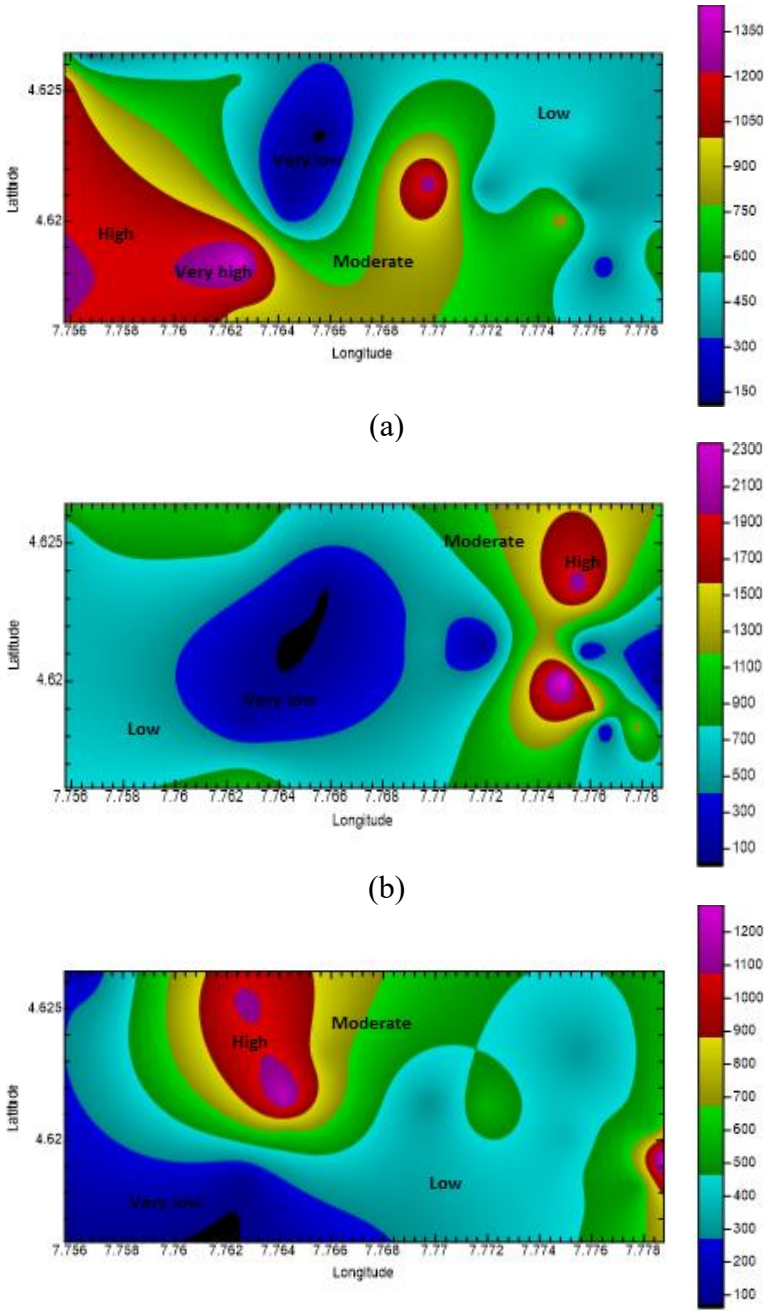

Figure 3: (a) Resistivity distribution of layer 1; (b): resistivity distribution of layer 2; (c) resistivity distribution of layer 3. On the color scale, blue represents very low, cyan represents low, green and yellow represent moderate, red represents high, and purple represents very high

According to Oladapo and Akintorinwa (2007), longitudinal conductance measures of less than 0.1 Ω^{-1} indicate poor aquifer protection, 0.1-0.19 Ω^{-1} indicates weak aquifer protection,0.2-0.69 Ω^{-1} indicates moderate aquifer protection, 0.7-4.9Ω^{-1} indicates good aquifer protection, 5-10 Ω^{-1} indicates very good aquifer protection, and > 10 Ω^{-1} indicates excellent aquifer protection. On the map of longitudinal conductance (Figure 5a), locations with high longitudinal conductance measures (> 0.75 Ω^{-1}) indicated zones with good aquifer protectivity. Figure 5a also indicated that most of the investigation area had weak aquifer protectivity, with good protectivity found predominantly in the north-central region.

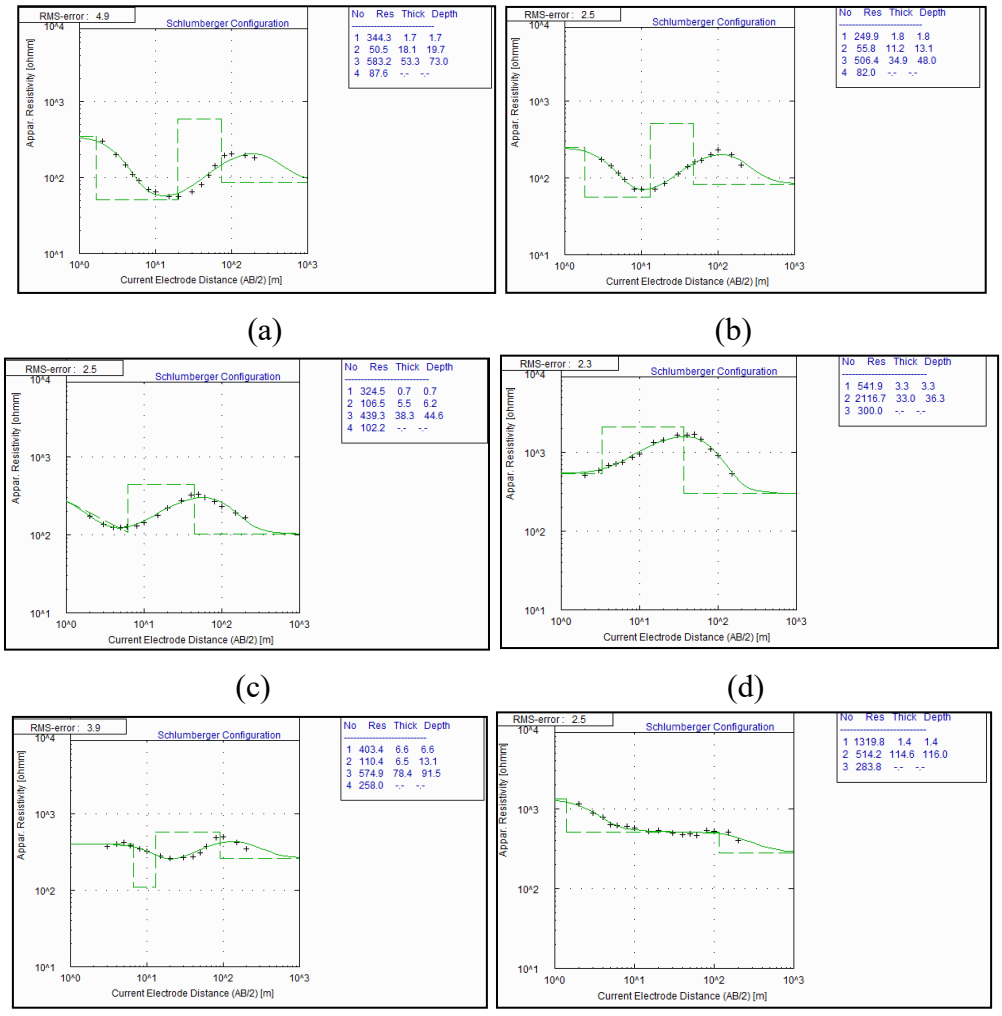

Figure 4(a-f): Representative curves generated from the VES interpretation

Table 2: Overview of second-order geo-electrical variables derived from the first-order geo-electrical indices

VES No.	Longitude	Latitude	Longitudinal conductance (Ω^{-1})			Transverse resistance (Ωm^2)			Resistivity gradient (Ω)			Reflection coefficient	
			Stratum 1	Stratum 2	Total	Stratum 1	Stratum 2	Total	Stratum 1	Stratum 2	Total	K_{12}	K_{23}
1	7.778767	4.619278	0.002	0.062	0.064	948.600	2214.810	3163.410	421.600	16.179	437.779	-0.539	0.751
2	7.77778	4.618333	0.002	0.003	0.005	514.400	4605.300	5119.700	514.400	375.943	890.343	0.438	-0.442
3	7.775753	4.620972	0.002	0.052	0.054	227.150	585.750	812.900	463.571	19.364	482.935	-0.506	0.610
4	7.778417	4.620472	0.016	0.059	0.075	2662.440	717.600	3380.040	61.121	16.985	78.106	-0.570	0.678
5	7.775583	4.623389	0.006	0.016	0.022	1788.270	69851.100	71639.370	164.212	64.142	228.355	0.592	-0.752
6	7.771917	4.621278	0.005	0.358	0.363	585.310	914.050	1499.360	202.529	2.790	205.319	-0.744	0.841
7	7.769833	4.621444	0.001	0.223	0.224	1847.720	58927.320	60775.040	942.714	4.487	947.201	-0.439	-0.289
8	7.774972	4.620083	0.001	0.013	0.014	842.000	79026.180	79868.180	842.000	78.148	920.148	0.494	-0.737
9	7.776528	4.618306	0.007	0.201	0.208	449.820	624.960	1074.780	138.833	4.982	143.815	-0.635	0.801
10	7.776234	4.618812	0.002	0.005	0.007	237.420	12380.090	12617.510	659.500	198.367	857.867	0.597	-0.509

11	7.7778251	4.624232	0.003	0.025	0.028	441.760	30481.000	30922.760	365.091	40.305	405.396	0.468	-0.394
12	7.762542	4.625431	0.002	0.078	0.080	619.740	72554.110	73173.85	512.182	12.864	525.046	0.263	0.072
13	7.764312	4.620323	0.005	0.107	0.112	164.790	49.220	214.01	203.444	9.304	212.749	-0.791	0.935
14	7.764213	4.621554	0.015	0.584	0.599	272.000	59.590	331.59	68.000	1.712	69.712	-0.862	0.984
15	7.765765	4.623312	0.016	0.898	0.913	142.800	69.520	212.32	63.467	1.114	64.581	-0.831	0.977
16	7.755764	4.625323	0.002	0.037	0.039	2143.200	14465.220	16608.42	593.684	27.108	620.792	-0.286	-0.432
17	7.756651	4.626434	0.006	0.014	0.020	402.600	17321.540	17724.14	178.933	69.386	248.319	0.607	-0.731
18	7.762621	4.618544	0.001	0.224	0.225	1902.810	1767.120	3669.93	1125.923	4.462	1130.385	-0.886	-0.013
19	7.762586	4.616121	0.003	0.016	0.019	2488.780	17962.560	20451.34	295.931	63.643	359.574	0.109	-0.873

This is worrisome, as groundwater resources are the main source of potable water in the investigated area. This map of longitudinal conductance has therefore given important information indicating that the north central area is most optimal for groundwater abstraction, and other locations should be avoided due to reduced aquifer protectivity in those areas.

Figure 5b illustrates the map of transverse resistance, the parameter employed to evaluate aquifer potentiality. The values of transverse resistance, with a gamut of 3669.93-79868.18Ωm^2 and a mean value of 20451.34 Ωm^2, indicated high aquifer potentiality. Locations with high transverse resistance measures (> 62000 Ωm) indicated zones with excellent aquifer potentiality.

The variation in resistivity gradient within the investigation area is portrayed in Figure 5c. The figure demonstrates that resistivity gradient measures varied widely within the region. Locations with very low/low resistivity gradient measures indicated zones with high aquifer protectivity. This occurred predominantly in the north-central section (i.e., zones with resistivity gradient values of 150 Ω and less). This implies that the majority of the study area had low susceptibility to contamination and was therefore prone to pollutant percolation via the vadose zone. The resistivity gradients in strata 1 and 2 and the total resistivity gradient for both strata were compared on regression curves (Figure 6).

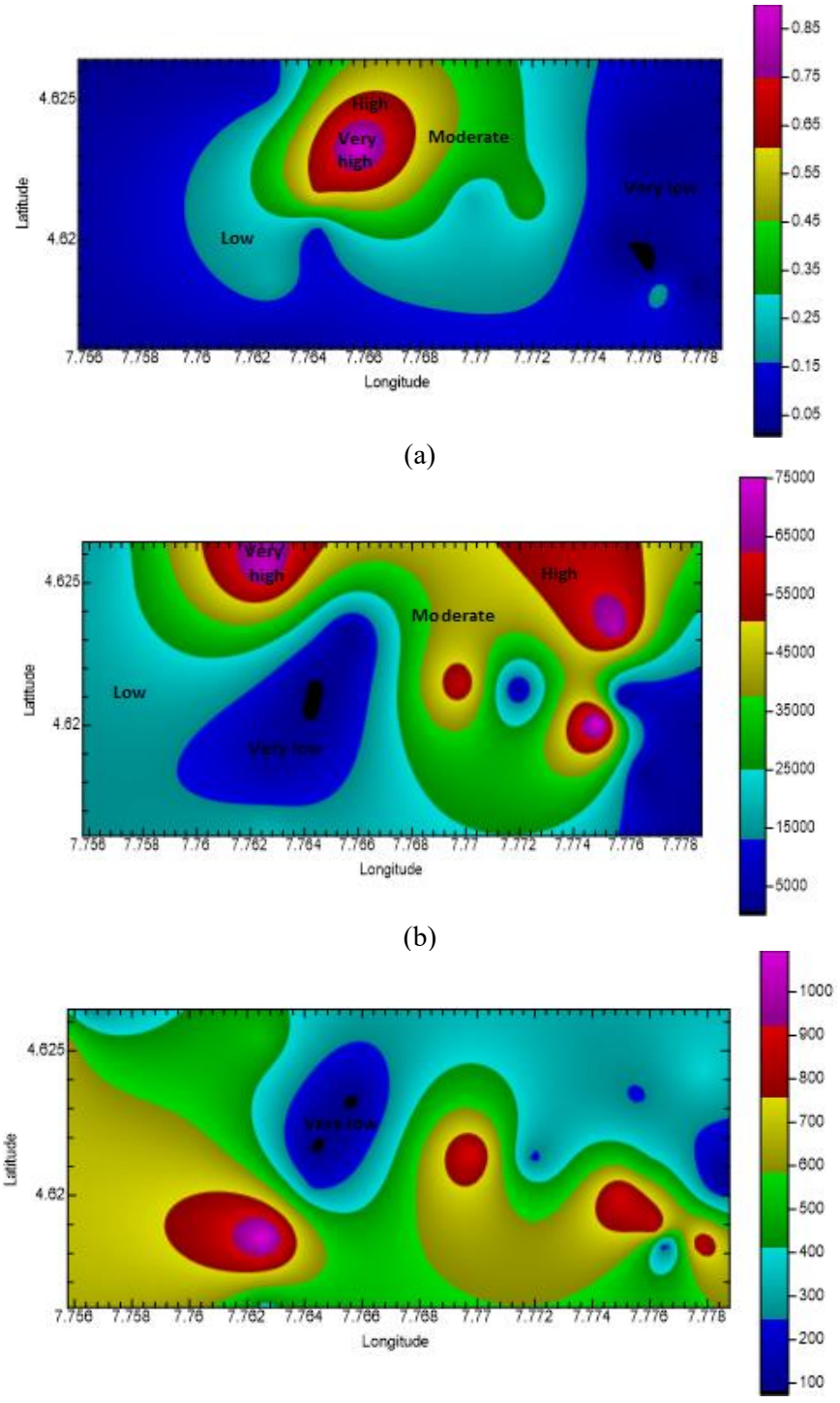

Figure 5(a): Map of longitudinal conductance; (b): map of transverse resistance; (c) map of resistivity gradient. On the color scale, blue represents very low, cyan represents low, green and yellow represent moderate, red represents high, and purple represents very high

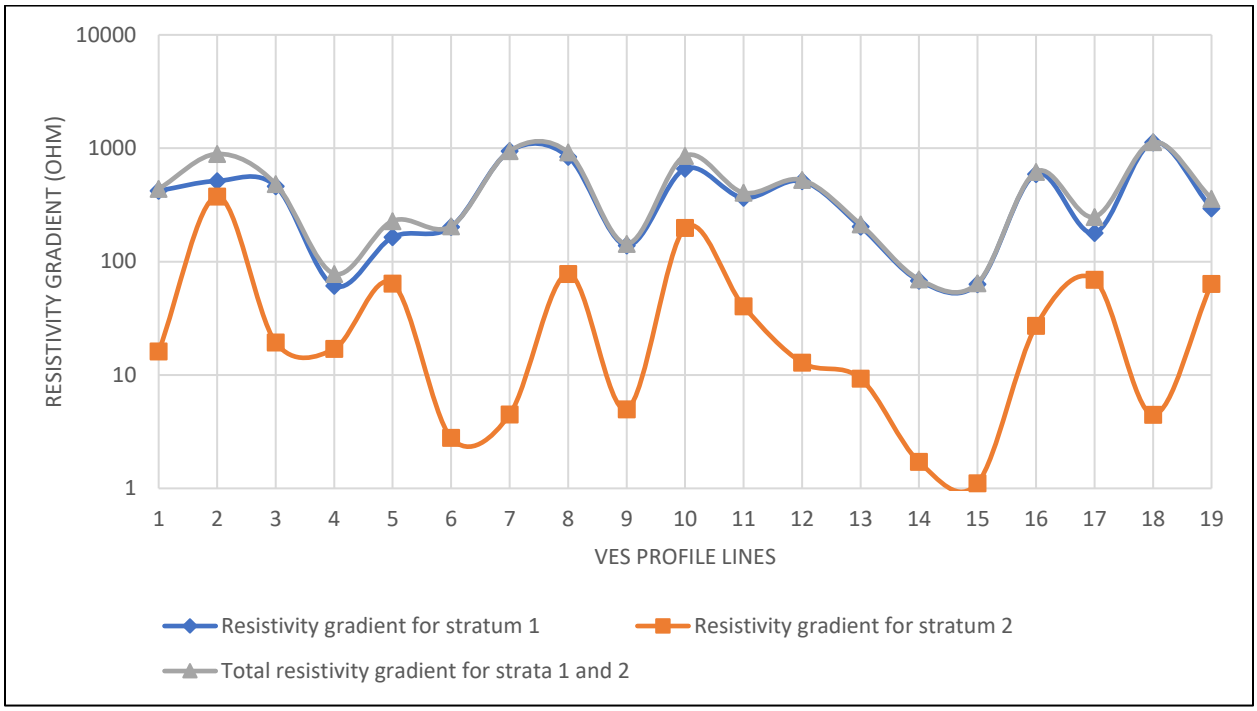

Figure 6: Regression curves illustrating individual resistivity gradient variation in strata 1 and 2. Also illustrated is the regression curve indicating the total resistivity gradient for strata 1 and 2

Figure 6 shows that the variability between resistivity gradient measures in stratum 2 was higher than that in stratum 1. This variability indicated that the subsurface would be more vulnerable to contaminant percolation due to the intercalation of diverse heterogeneous earth materials. The typically homogenous geo-layers that would help preclude leakage of contamination were mostly non-existent, making it more likely that toxicants would easily percolate the vadose zone into the aquifer material. Via observations of the degree of variability in subsurface resistivity gradient measures, one could deduce the degree of susceptibility of the water-bearing formation to pollution. Extremely variable subsurface layers indicated lithologies more prone to contamination. Figure 7 illustrates the difference curve of resistivity gradients between layers 1 and 2. A wide variation was observed in the difference curve, indicating greater vulnerability to contamination. To corroborate the wide variations in subsurface resistivity generated from the resistivity gradient regression curves, electrical resistivity tomograms (Figures 8a-d) generated from electrical resistivity tomography surveys were analyzed. The electrical resistivity tomograms indicated large subsurface heterogeneity, the result of intercalations of heterogeneous material within the study area. These wide resistivity variations led to reduced subsurface homogeneity, resulting in reduced protectivity of the subsurface strata against percolation by toxicants.

Other measures to evaluate subsurface resistivity heterogeneity were the electrical reflection coefficient connecting strata 1 and 2 (K_{12}), and the electrical reflection coefficient connecting strata 2 and 3 (K_{23}). Figures 9a and 9b illustrate iso-parametric maps for K_{12} and K_{23} respectively. These measures of K_{12} and K_{23} showed wide subsurface resistivity variability, another indication of a heterogeneous overburden with lithofacies changes within the geo-stratigraphic units. Comparing the regression plots of K_{12} and K_{23} yielded Figure 10.

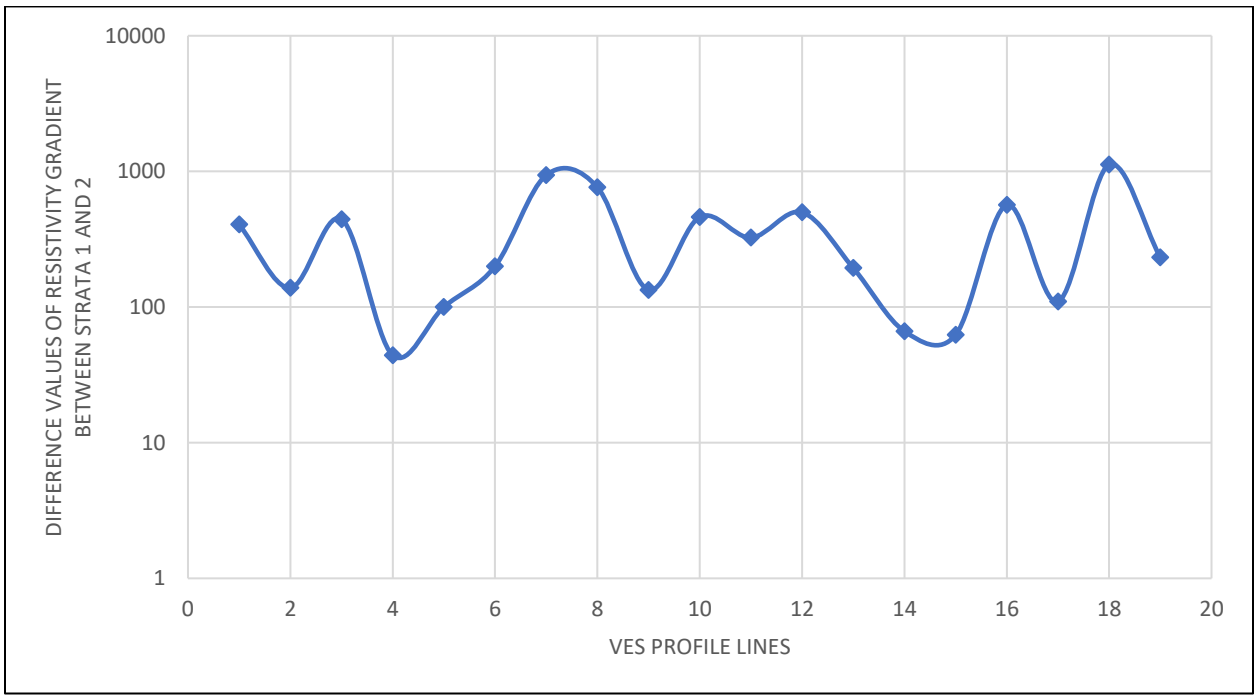

Figure 7: Regression curve illustrating the difference values of resistivity gradients between strata 1 and 2

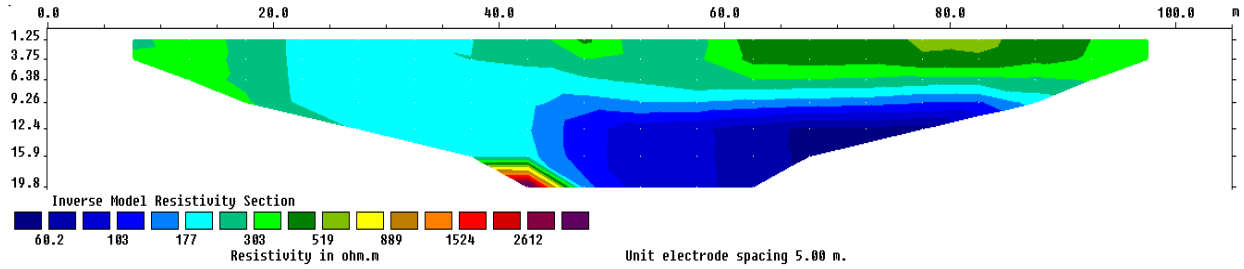

(a)

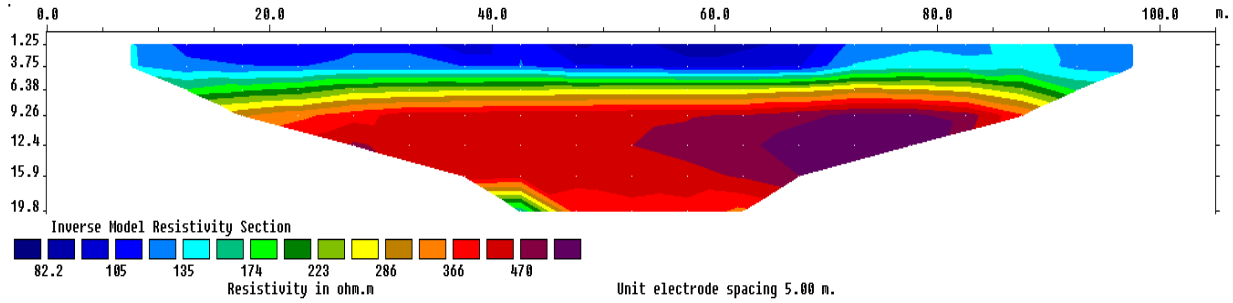

(b)

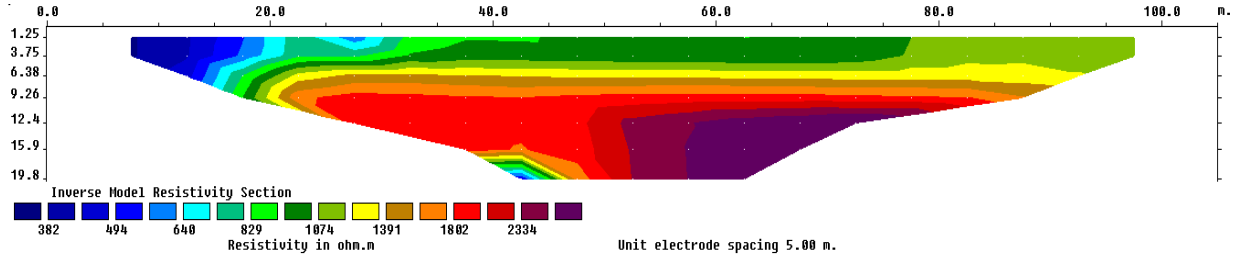

(c)

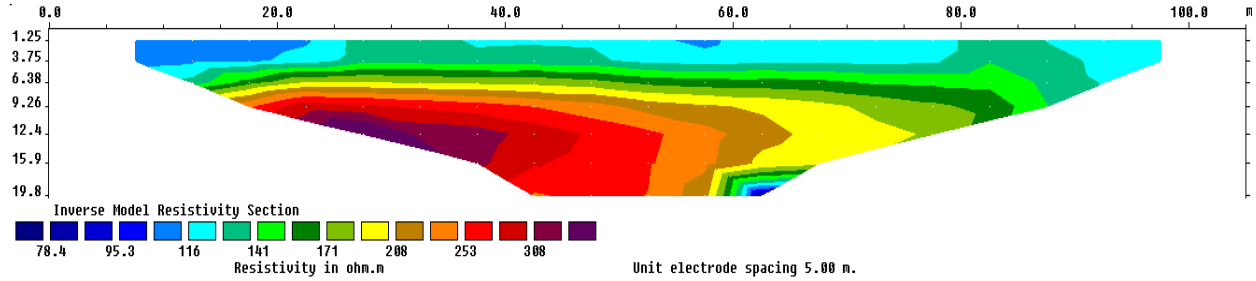

(d)

Figure 8a-d: Representative resistivity tomograms generated from four ERT profile lines

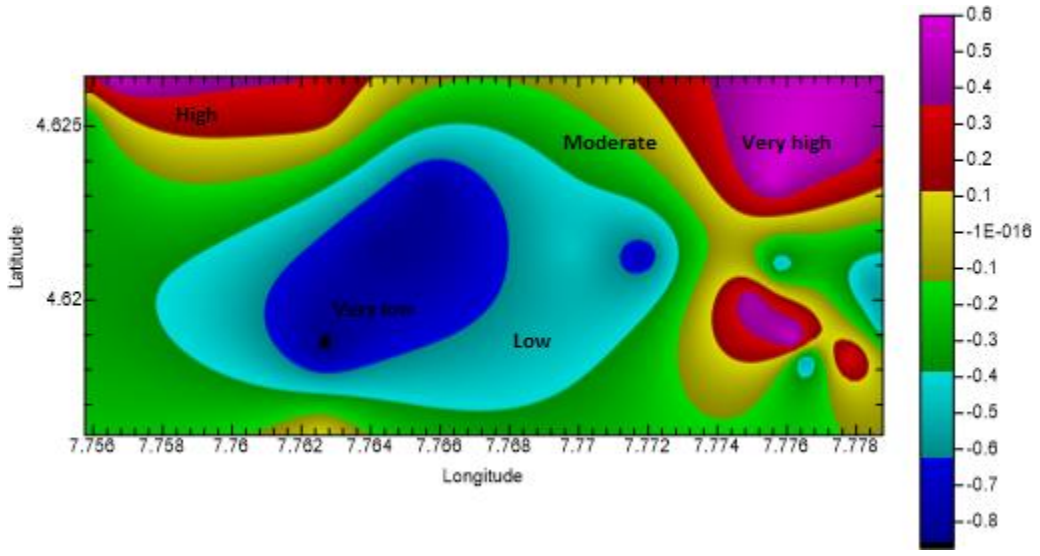

(a)

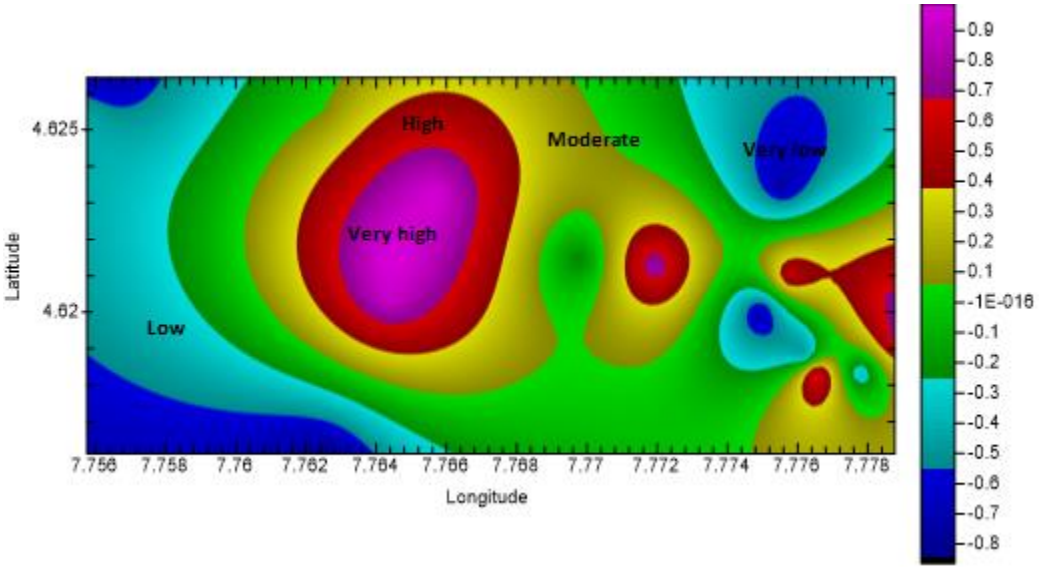

(b)

Figure 9: (a) Electrical reflection coefficient between strata1 and 2 (K_{12}). (b) Electrical reflection coefficient between strata 2 and 3 (K_{23}). For this investigation area, the color scale indicated in these figures represents varying measures of the electrical reflection coefficient. Blue represents very low, cyan represents low, green and yellow represent moderate, red represents high, and purple represents very high.

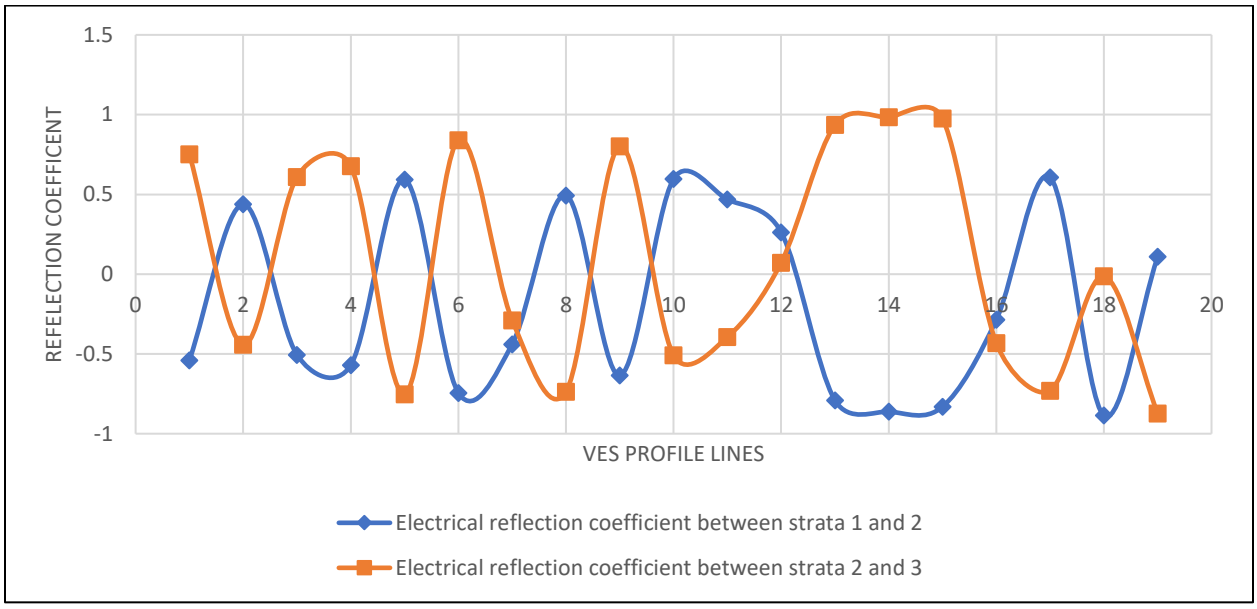

Figure 10: Regression plots of the electrical reflection coefficient between strata 1 and 2 (K_{12}), and the electrical reflection coefficient between strata 2 and 3 (K_{23}).

The regression curves of K_{12} and K_{23} in Figure 10 were observed to be out of phase with one another, indicating alternating inter-beddings of diverse lithological facies, in this case, arenites and argillites. These measures of the second-order geoelectrical indices have therefore indicated that the lithofacies are highly heterogeneous, that the groundwater protectivity is generally weak, and that the aquifer is prolific.

6.0 Conclusion

Geoelectrical technology was employed to investigate electrical resistivity gradient measures in a bid to characterize subterranean heterogeneity and aquifer vulnerability to contamination. Nineteen vertical electrical soundings and four electrical resistivity tomography profile lines were investigated. The topmost lithological stratum (heterogenous topsoil) had resistivity measures of 95.2 - 1463.7 Ωm, with a thickness of 0.6 m - 6.6 m; the second lithological stratum (mix of clay and sand) had resistivity measures of 8.8 Ωm - 2485.1 Ωm with a thickness of 2.3m -114.6 m, and the third lithological stratum (fine/medium-grained sands) had resistivity measures of 72.5 Ωm - 1332.7 Ωm with a thickness 34.9m – 123.7 m. Vertical electrical sounding data were interpreted to generate second-order geoelectrical indices such as electrical resistivity gradient, electrical reflection coefficient, longitudinal conductance, and transverse resistance. The resistivity gradient values fluctuated from low to high, delineating highly heterogeneous litho-facies and diverse resistivity curve types. Mean values of resistivity gradients for layers 1 and 2 were 411.42Ω and 53.22Ω respectively. The integration of resistivity gradient measures with other second-order geo-electrical parameters such as electrical reflection coefficient, longitudinal conductance, and transverse resistance yielded key information for parameterizing subterranean heterogeneity, assessing geologic lithologies, and characterizing the aquifer's susceptibility to degradation. The electrical reflection coefficient between strata 1 and 2, and that between strata 2 and 3, were observed to be 90^o out of phase with one another, indicating alternating inter-beddings of diverse lithological facies. The map of resistivity gradient and longitudinal conductance indicated that subterranean water protectivity was generally

poor. The map of transverse resistance indicated that subterranean water potential was high. The integration of electrical resistivity gradient with other geo-electrical measures has generated key geo-hydraulic information for parameterizing subterranean heterogeneity and groundwater vulnerability to contamination.

Data Availability

The authors confirm that the data supporting the findings of this study are available within the article and its supplementary materials.

Competing Interests Statements

The authors declare that they have no known competing financial interests or personal relationships that could have appeared to influence the work reported in this paper.

References

Adebiyi, A.D., Ilugbo, S.O., Bamidele, O.E. and Egunjobi, T., 2019. Assessment of aquifer vulnerability using multi-criteria decision analysis around Akure Industrial Estate, Akure, Southwestern Nigeria. *Journal of Engineering Research and Reports*, *3*(3), pp.1-13. https://doi.org/10.9734/jerr/2018/-v3i316874.

Adeniji, A.E., Omonona, O.V., Obiora, D.N. and Chukudebelu, J.U., 2014. Evaluation of soil corrosivity and aquifer protective capacity using geoelectrical investigation in Bwari basement complex area, Abuja. *Journal of Earth System Science*, *123*, pp.491-502. https://doi.org/10.1007/s12040-014-0416-1.

Agbasi, O.E., Aziz, N.A., Abdulrazzaq, Z.T. and Etuk, S.E., 2019. Integrated geophysical data and GIS technique to forecast the potential groundwater locations in part of South Eastern Nigeria. *Iraqi Journal of Science*, *60*(5), pp.1013-1022. https://doi-.org/10.24996/ijs.2019.60.5.11.

Aizebeokhai, A.P. and Oyebanjo, O.A., 2013. Application of vertical electrical soundings to characterize aquifer potential in Ota, Southwestern Nigeria. *International Journal of Physical Sciences*, *8*(46), pp.2077-85. https://doi.org/10.1190/segam-2018-2990105.1.

Akiang, F.B., Amah, E.T., George, A.M., Okoli, E.A., Agbasi, O.E. and Iwuoha, P.O., 2024. Hydrogeological assessment and groundwater potential study in Calabar South Local Government Area: a vertical electrical sounding (VES) approach. *International Journal of Energy and Water Resources*, pp.1-13. https:-//doi.org/10.1007/s4210802-4-00279-y.

Alao, J.O., Lawal, K.M., Dewu, B.B.M. and Raimi, J., 2024. Detection of shallow underground targets using electrical resistivity tomography and the implications in civil/ environmental engineering. *Discover Geoscience*, *2*(1), p.52. https://doi.org/10.1007-/s44288-024-00058-6.

Arowoogun, K.I. and Osinowo, O.O., 2022. 3D resistivity model of 1D vertical electrical sounding (VES) data for groundwater potential and aquifer protective capacity assessment: A case study. *Modeling Earth Systems and Environment*, *8*(2), pp.2615-2626. https://doi.org/10.1007/s40808-021-01254-w

Asfahani, J., 2023a. Geo-electrical investigation for characterizing the shallow Quaternary aquifer parameters and vulnerability to contamination: A case study from semi-arid Khanasser Valley region, Syria. *Water*

Practice and Technology, 18(7), 1639-1662.https://doi.org/10.2166/wpt.2023.084.

Asfahani, J., 2023b. The influence of geoelectrical parameters on the Quaternary aquifer and its protectivity and contamination: A case study from the Khanasser Valley Region, Northern Syria. *Water Practice and Technology*, 18 (12), 3235 – 3254. https://-doi.org/10.2166/wpt.2023.212.

Atakpo, E.A. and Ayolabi, E.A., 2009. Evaluation of aquifer vulnerability and the protective capacity in some oil producing communities of western Niger Delta. *The Environmentalist*, *29*, pp.310-317. https://doi.org/-10.1007/s10669-008-9191-3.

Avbovbo, A.A., 1978. Tertiary lithostratigraphy of Niger delta. *AAPG Bulletin*, 62(2), 295–300. https://doi.org/10.1306/c1ea482e16c9-11d7-8645000102c1865d.

Aweto, K.E., 2011. Aquifer vulnerability assessment at Oke-Ila area, southwestern Nigeria. *International Journal of the Physical Sciences*, 6(33), 7574–7583. https://doi.org/10.9734/jgeesi/2018/41836.

Baki, A.M., Ghavami, S.M., Qureshi, S.A.M. and Ghaffari, O., 2024. A three-step modification of the DRASTIC model using spatial multi criteria decision making methods to assess groundwater vulnerability. *Groundwater for Sustainable Development*, *26*, p.101277. https://doi.org-/10.1016/j.gsd.2024.101277.

Batte, A. G., Barifaijo, E., Kiberu, J.M., Kawule, W., Muwanga, A., Owor, M., and Kisekulo, J., 2010. Correlation of geoelectric data with aquifer parameters to delineate the groundwater potential of hard rock terrain in Central Uganda. *Pure and Applied Geophysics*, 167, 1549–1559. https://-doi.org/10.1007/s00024-010-0109-x.

Bertero, M., Boccacci, P. and De Mol, C., 2021. *Introduction to inverse problems in imaging*. CRC press, Boca Raton, Florida.

Braga, A.C.D.O. and Francisco, R.F., 2014. Natural vulnerability assessment to contamination of unconfined aquifers by longitudinal conductance – (S) method. *Journal of Geography and Geology*, *6*(4), pp.68-79. https://doi.org/-10.5539/jgg.v6n4p68.

Chandra, S., Ahmed, S., Ram, A. and Dewandel, B., 2008. Estimation of hard rock aquifers hydraulic conductivity from geoelectrical measurements: a theoretical development with field application. *Journal of Hydrology*, *357* (3-4), pp.218-227. https://doi.org/10.1016/-j.jhydrol.2008.05.023.

Choudhury, K., Saha, D.K., and Chakraborty, P., 2001. Geophysical study for saline water intrusion in coastal alluvial terrain. *Journal of Applied Geophysics*, 46(3), 189–200. https://doi.org/10.1016/s09269851(01)00038-6.

Civita M., 1994. Civita M., 1994. Le Carte della vulnerabilit`a degli acquiferi all'inquinamento: Teoria & pratica [Aquifer vulnerability to pollution maps: theory and practice]. Pitagora, Bologna, Italy.

Dauda, G. and Ali, A.M., 2024. Delineating leachate-groundwater interaction at Gyadi-Gyadi dumpsite, Kano, using natural electromagnetic (EM) field detector and Vertical Electrical Sounding (VES). *Geosystems and Geoenvironment*, *3*(4), p.100303. https://doi.org-/10.1016/j.geogeo.2024.100303.

Edet, A.E., 2004. Vulnerability evaluation of a coastal plain sand aquifer with a case example from Calabar, southeastern Nigeria. *Environmental Geology*, 45, 1062–1070. https://doi.org/10.1007/s00254-004-0964-9.

Ebong, E. D., Emeka, C.N., Melouah, O., Illa Ullah, R., Ita, A.E. and Asfahani, J., 2023. Delineation of groundwater potential zones using electrical resistivity technique in Obudu basement terrain of Cross River State, southeastern Nigeria. *Water Practice and Technology*, 18(11), 2884–2900. https://doi.org/10.2166/wpt.2023.174.

Ejiogu, B.C., Opara, A.I., Nwosu, E.I., Nwofor, O.K., Onyema, J.C. and Chinaka, J.C., 2019. Estimates of aquifer geo-hydraulic and vulnerability characteristics of Imo State and environs, Southeastern Nigeria, using electrical conductivity data. *Environmental Monitoring and Assessment*, 191, 1–19. https://doi.org/10.1007/s10661-019-7335-1.

Ekanem, A.M. and Udosen, N.I., 2023a. Hydrogeochemical–geophysical investigations of groundwater quality and susceptibility potential in Ikot Ekpene – Obot Akara Local Government Areas, Southern Nigeria. *Water Practice & Technology*, 18(11), pp.2675-2704. https://doi.org/10.2166/wpt.2023.187.

Ekanem, A.M. and Udosen, N.I., 2023b. Evaluation of Groundwater Potentiality and Quality in Ikot Ekpene-Obot Akara Local Government Areas, Southern Nigeria. *Environmental Contaminants Reviews*, 6(1): 46-57. https://doi.org/10.26480/ecr.01.2023.46.57.

Eke, D.R., Opara, A.I., Inyang, G.E., Emberga, T.T., Echetama, H.N., Ugwuegbu, C.A., Onwe, R.M., Onyema, J.C. and Chinaka, J.C., 2015. Hydrogeophysical evaluation and vulnerability assessment of shallow aquifers of the Upper Imo River Basin, Southeastern Nigeria. *American Journal of Environmental Protection*, 3(4), 125–136.

Ekwe, A.C. and Opara, A.I., 2012. Aquifer transmissivity from surface geo-electrical data: A case study of Owerri and environs, southeastern Nigeria. *Journal of the Geological Society of India*, 80, 123–128. https://doi.org/10.1007/s12594-012-0126-8.

Ekwe, A.C., Opara, A.I., Okeugo, C.G., Azuoko, G.B., Nkitnam, E.E., Abraham, E. M., Chukwu, C. G. and Mbaeyi, G., 2020. Determination of aquifer parameters from geosounding data in parts of Afikpo Sub-basin, southeastern Nigeria. *Arabian Journal of Geosciences*, 13, 1–15. https://doi.org/10.1007/s12517-020-5137-y.

Emmanuel, C.C. 2013. Monitoring the Quality of Groundwater and Leachate Contamination near Waste Dump in Coastal Plain Sand Aquifer. M.Sc. Thesis, University of Calabar, Calabar.

Engl, H.W., Hanke, M. and Neubauer, A., 1996. Regularization of Inverse Problems. Mathematics and Its Applications, Vol. 375, Kluwer Academic Publishers Group, Dordrecht.

Eyankware, M.O. and Aleke, G., 2021. Geoelectric investigation to determine fracture zones and aquifer vulnerability in southern Benue Trough southeastern Nigeria. *Arabian Journal of Geosciences*, 14(22), 2259. https://doi.org/10.1007/s12-517-021-08542-w.

Eyankware, M.O., Ogwah, C. and Selemo, A.O., 2020. Geoelectrical parameters for the estimation of groundwater potential in fracture aquifer at sub-urban area of Abakaliki, SE Nigeria. *International Journal of Earth Science and Geophysics*, 6(031), 2-15. https://doi.org/10.35840/26-31-5033/1831.

Foster, S.S.D., 1987. Fundamental concepts in aquifer vulnerability, pollution risk and protection strategy. In: van Duijvanbooden, W., van Waegeningh, H.G. (Eds.), Vulnerability of soil and groundwater to pollution. TNO Committee on Hydrological Research, Delft, The Netherlands.

Frifita, N., Mickus, K., Ben-Zaied, M., Bouajila, A., Mahmoudi, S. and Ouessar, M., 2024. Geophysical contribution using electrical resistivity to study the Triassic sandstone aquifer, southeastern Tunisia. *Journal of African Earth Sciences*, *210*, p.105165. https://doi.org/10.1016/j.jafrearsci.2023.105165.

George, N. J., 2021. Modelling the trends of resistivity gradient in hydrogeological units: a case study of alluvial environment. *Modeling Earth Systems and Environment*, 7, pp.95-104. https://doi.org-/10.1007/s40808-020-01021-3.

George, N.J., Ibuot, J.C., Ekanem, A.M. and George, A.M., 2018. Estimating the indices of inter-transmissibility magnitude of active surficial hydrogeologic units in Itu, Akwa Ibom State, Southern Nigeria. *Arabian Journal of Geosciences*, 11, pp.1-16. https://doi.org-/10.1007/s12517-018-3475-9.

George, N.J., 2020. Appraisal of hydraulic flow units and factors of the dynamics and contamination of hydrogeological units in the littoral zones: a case study of Akwa Ibom State University and its Environs, Mkpat Enin LGA, Nigeria. *Natural Resources Research*, 29(6), pp.3771-3788. https://doi.org/10.1007/s11053-020-09673-9.

George, N.J., Ekanem, A.M., Ibanga, J.I. and Udosen, N.I., 2017. Hydrodynamic implications of aquifer quality index (AQI) and flow zone indicator (FZI) in groundwater abstraction: a case study of coastal hydro-lithofacies in South-eastern Nigeria. *Journal of Coastal Conservation*, 21, pp.759-776. https://doi.org/10.1007-/s11852-017-0535-3.

George, N.J., Ekanem, K.R., Ekanem, A.M., Udosen, N.I. and Thomas, J.E., 2022. Generic comparison of ISM and LSIT interpretation of geo-resistivity technology data, using constraints of ground truths: a tool for efficient explorability of groundwater and related resources. *Acta Geophysica*, 70(3), pp.1223-1239. https://-doi.org/10.1007/s11600-022-00794-8.

George, N.J., Ekanem, A.M., Thomas, J.E., Udosen, N.I., Ossai, N.M. and Atat, J.G., 2024. Electro-sequence valorization of specific enablers of aquifer vulnerability and contamination: A case of index-based model approach for ascertaining the threats to quality groundwater in sedimentary beds. *HydroResearch*, 7, pp.71-85. https://doi.-org/10.1016/j.hydres.2023.11.006.

Groetsch, C.W. and Groetsch, C.W., 1993. *Inverse problems in the mathematical sciences* (Vol. 52). Braunschweig: Vieweg.

Ibuot, J.C. and Obiora, D.N., 2021. Estimating geohydrodynamic parameters and their

implications on aquifer repositories: A case study of University of Nigeria, Nsukka, Enugu State. *Water Practice and Technology*, 16(1), 162-181. https://doi.org/10.2166/wpt-.2020.105.

Ibuot, J.C., Omeje, E.T. and Obiora, D.N., 2021. Geophysical evaluation of geohydrokinetic properties of aquifer units in parts of Enugu state, Nigeria. *Water Practice and Technology*, 16(4), 1397–1409. https://doi.org/10.2166-/wpt.2021.074.

Inim, I.J., Udosen, N.I., Tijani, M.N., Affiah, U.E. and George, N.J., 2020. Time-lapse electrical resistivity investigation of seawater intrusion in coastal aquifer of Ibeno, Southeastern Nigeria. *Applied Water Science*, 10(11), pp.1-12. https://doi.org/-10.1007/s13201-020-01316-x.

Inyang, N.E., Ehibor, I.U., Ekot, A.E., and Udo, I.G., 2024. An environmental assessment and a priori implications of field investigations of older MSW at Uyo and Younger MSW at Eket, Akwa Ibom State, southern Nigeria. *Researchers Journal of Science and Technology*, *4*(1), 45–71.

Ishak, M.F., Zolkepli, M.F., Masyhur, E.M.H., Yunus, N.Z.M., Rashid, A.S.A., Hezmi, M.A., Hasbollah, D.Z.A. and Yusoff, A.R., 2022. Interrelationship between borehole lithology and electrical resistivity for geotechnical site investigation. *Physics and Chemistry of the Earth*, Parts A/B/C, 128, p.103279. https://doi.org/10.1016/j.pce.20-22.103279.

Jamaa, H., Hamdouni, T., El Achheb, A. and Ibno Namr, K., 2024. Assessment of groundwater vulnerability to contamination using the DRASTIC model and GIS functions in Doukkala Plain, Morocco. *Modeling Earth Systems and Environment*, *10*(1), pp.1-17. https://doi.org/10.1007/s40808-02301789-0

Kenneth, S.O. and Ebifuro, O., 2012. Geoelectric sounding for the determination of aquifer transmissivity in parts of Bayelsa State, South South Nigeria. *Journal of Water Resource and Protection*, *2012*. https://doi.org/10.423-6/jwarp.2012.46039.

Lobo-Ferreira, J.P., Chachadi A.G., Diamantino, C. and Henriques, M.J., .2007. Assessing aquifer vulnerability to seawater intrusion using the GALDIT method: part 1, application to the Portuguese Monte Gordo aquifer. In: Lobo-Ferreira J.P. and Viera J.M.P. (eds) Proceedings water in Celtic countries: quantity, quality and climate variability, IAHS Publication 310, International Association of Hydrological Sciences, Wallingford, UK, pp 161–171.

Loke, M.H. and Dahlin, T., 2002. A comparison of the Gauss–Newton and quasi-Newton methods in resistivity imaging inversion. *Journal of Applied Geophysics*, 49(3), 149–162. https://doi.org/10.1016/s09269851(01-)00106-9.

Loke, M.H., Acworth, I. and Dahlin, T., 2001. A comparison of smooth and blocky inversion methods in 2-D electrical imaging surveys. *ASEG Extended Abstracts,* 2001(1), 1–4. https://doi.org/10.1071/aseg2001ab075.

Loke, M. H. and Barker, R. D., 1996. Rapid least-squares inversion of apparent resistivity pseudosections by a quasi-Newton method. *Geophysical Prospecting*, 44(1), 131–152. https://doi.org/10.1111/j.1365-2478.1996.tb00142.x.

Mehta, D., Patel, P., Sharma, N. and Eslamian, S., 2024. Comparative analysis of DRASTIC

and GOD model for groundwater vulnerability assessment. *Modeling Earth Systems and Environment*, *10*(1), pp.671-694. https://doi.org/10.1007/s40808-023-01795-2.

Mohammed, M.A., Szabó, N.P. and Szűcs, P., 2023a. Exploring hydrogeological parameters by integration of geophysical and hydrogeological methods in northern Khartoum state, Sudan. *Groundwater for Sustainable Development*, *20*, p.100891. https://doi.org/10.1016/j.gsd.2022.100891.

Mohammed, M.A., Szabó, N.P. and Szűcs, P., 2023b. Characterization of groundwater aquifers using hydrogeophysical and hydrogeochemical methods in the eastern Nile River area, Khartoum State, Sudan. *Environmental Earth Sciences*, *82*(9), p.219. https://doi.org/10.1007/s126650231-0915-1.

Mohan, S., Muralimohan, N. and Vidhya, K., 2024, January. Contamination of Groundwater Assessment in Hard Rock Aquifer by Using Geographic Information System (Drastic Model) in the Thirumanimuthar Sub-basin, South India. In *Doklady Earth Sciences* (Vol. 514, No. 1, pp. 149-160). Moscow: Pleiades Publishing. https://doi.org/10.1134/s1028334x23601700.

Naidu, S., Gupta, G., Shailaja, G. and Tahama, K., 2021. Spatial behavior of the Dar-Zarrouk parameters for exploration and differentiation of water bodies aquifers in parts of Konkan coast of Maharashtra, India. *Journal of Coastal Conservation*, *25*, pp.1-9. https://doi.org/10.1007/s11852-021-00807-6.

Ndatuwong, L.G. and Yadav, G.S., 2015. Application of geo-electrical data to evaluate groundwater potential zone and assessment of overburden protective capacity in part of Sonebhadra district, Uttar Pradesh. *Environmental Earth Sciences*, *73*, pp.3655-3664. https://doi.org/10.1007/s12-665-014-3649-z.

Nisar, U.B., Khan, M.J., Imran, M., Khan, M.R., Farooq, M., Ehsan, S.A., Ahmad, A., Qazi, H.H., Rashid, N. and Manzoor, T., 2021. Groundwater investigations in the Hattar industrial estate and its vicinity, Haripur district, Pakistan: An integrated approach. *Kuwait Journal of Science*, *48*(1). https://doi.org/-10.48129/kjs.v48i1.7820.

Obiora, D.N., Ajala, A.E. and Ibuot, J.C., 2015. Investigation of groundwater flow potential in Makurdi, North Central Nigeria, using surficial electrical resistivity method. *African Journal of Environmental Science and Technology*, *9*(9), pp.723-733. https://doi.-org/10.5897/ajest2015.1983.

Obiora, D.N., Ibuot, J.C. and George, N.J., 2016. Evaluation of aquifer potential, geoelectric and hydraulic parameters in Ezza North, southeastern Nigeria, using geoelectric sounding. *International Journal of Environmental Science and Technology*, *13*, pp.435-444. https://doi.org/10.1007/s13762-01508-86-y.

Ojo, O. A., Oladimeji, R.G., Alabi, R.O., Ejiwale, I.R., Babafemi, E.O., Akinyele, F.O., and Faleye, E.T., 2024. Geoelectrical and geotechnical based-assessment of sub-surface soil electrical earthening property and corrosive vulnerability along Coker Village Road, Osogbo, Nigeria. *Researchers Journal of Science and Technology*, *4*(4), 1–21.

Okoroh, D.O. and Ibuot, J.C., 2022. Hydrogeochemical assessment of groundwater

quality: A case study of Federal College of Education (Technical), Omoku, Rivers State. *Water Practice and Technology*, 17(7), 1458–1469. https://doi.org/10.2166-/wpt.2022.077.

Oladapo, M.I., Mohammed, M.Z., Adeoye, O.O. and Adetola, B.A., 2004. Geoelectrical investigation of the Ondo State housing corporation estate Ijapo Akure, South-western Nigeria. *Journal of Mining and Geology*, 40(1), 41–48. https://doi.org-/10.4314/jmg.v40i1.18807.

Olorunfemi, M.O., Oni, A.G., Fadare, T.K. and Olajuyigbe, O.E., 2024. Assessment of subsoil characteristics by electrical resistivity method for engineering, groundwater and environmental impact at a proposed estate in a basement complex terrain—a case study from Southwestern Nigeria. *Arabian Journal of Geo-sciences*, *17*(7), p.220. https://doi.org/10-.1007/s12517-024-12017-z.

Oloruntola, M.O., Bayewu, O.O., Mosuro, G.O., Folorunso, A.F. and Ibikunle, S.O., 2017. Groundwater occurrence and aquifer vul-nerability assessment of Magodo Area, Lagos, Southwestern Nigeria. *Arabian Journal of Geosciences*, 10, 1–13. https://doi.org/10.1007/s12517-017-2914-3.

Oni, T.E., Omosuyi, G.O. and Akinlalu, A.A., 2017. Groundwater vulnerability assessment using hydrogeologic and geoelectric layer susceptibility indexing at Igbara Oke, Southwestern Nigeria. *NRIAG Journal of Astronomy and Geophysics*, *6*(2), pp.452-458. https://doi.org/10.1016/j.nrjag.2017.0-4.009.

Onuoha, K.M. and Mbazi, F.C., 1988. Aquifer transmissivity from electrical sounding data: The case of Ajali Sandstone aquifers southwest of Enugu, Nigeria. In: Groundwater and Mineral Resources of Nigeria. Vieweg, Braunschweig, Germany, pp. 17–29. https:-//doi.org/10.1007/978-3-322-87857-1_3.

Opara, A.I., Edward, O.O., Eyankware, M.O., Akakuru, O.C., Oli, I.C. and Udeh, H.M., 2023. Use of geo-electric data in the determination of groundwater potentials and vulnerability mapping in the southern Benue Trough Nigeria. *International Journal of Environmental Science and Technology*, 20(8), 8975–9000. https://doi.org/10.1007-/s13762-022-04485-1.

Ourarhi, S., Barkaoui, A.E., Zarhloule, Y., Kadiri, M. and Bouiss, H., 2024. Groundwater vulnerability assessment in the Triffa Plain based on GIS combined with DRASTIC, SINTACS, and GOD models. *Modeling Earth Systems and Environment*, *10*(1), pp.619-629. https://doi.org/10.1007/s4080-8-023-01801-7.

Petters, S.W., Usoro, E.J., Udo, E.J., Obot, U.W. and Okpon, S. N., 1989. Akwa Ibom State: Physical background, soils and land use and ecological problems. Govt. Print Office, Uyo, p. 603.

Rai, S.N., Thiagarajan, S., Kumari, Y.R., Rao, V.A. and Manglik, A., 2013. Delineation of aquifers in basaltic hard rock terrain using vertical electrical soundings data. *Journal of Earth System Science*, 122, 29–41. https:-/doi.org/10.1007/s12040-012-0248-9.

Reijers, T.J.A. and Petters, S.W., 1987. Depositional environments and diagenesis of Albian carbonates on the Calabar Flank, SE Nigeria. *Journal of Petroleum Geology*, 10(3), pp.283-294. https://doi.org-/10.1111/j.1747-5457.1987.tb00947.x.

Richter, M., 2021. *Inverse problems: Basics, theory and applications in geophysics*. Springer Nature. Switzerland.

Saha, D. and Alam, F., 2014. Groundwater vulnerability assessment using DRASTIC and Pesticide DRASTIC models in intense agriculture area of the Gangetic plains, India. *Environmental Monitoring and Assessment*, 186, 8741–8763. https://doi.-org/-10.1007/s10661-014-4041-x.

Samouëlian, A., Cousin, I., Tabbagh, A., Bruand, A. and Richard, G., 2005. Electrical resistivity survey in soil science: a review. *Soil and Tillage research*, *83*(2), pp.173-193. https://doi.org/10.1016/j.still.2-004.10.004.

Sankar, K., Karunanidhi, D., Kalaivanan, K., Subramani, T., Shanthi, D. and Balamurugan, P., 2023. Integrated hydro-geophysical and GIS based demarcation of groundwater potential and vulnerability zones in a hard rock and sedimentary terrain of Southern India. *Chemosphere*, *316*, p.137305. https://doi.org/10.1016/j.chem-osphere.2022.137305.

Sathiyamoorthy, M. and Ganesan, M., 2018. Delineation of groundwater potential and recharge zone using electrical resistivity method around Veeranam Tank, Tamil Nadu, India. *Journal of the Institution of Engineers (India): Series A*, *99*, pp.637-645. https://doi.org/10.1007/s40030-018-0318-3.

Short, K. C. and Stauble, A. J., 1967. Outline of geology of Niger Delta. *AAPG Bulletin*, 51(5), 761–779. https://doi.org/10.1306-/5d25c0cf-16c1-11d7-8645000102c1865d.

Sikandar, P. and Christen, E. W., 2012. Geoelectrical sounding for the estimation of hydraulic conductivity of alluvial aquifers. *Water Resources Management*, 26(5), 1201–1215. https://doi.org/10.1007/s11269-011-9954-3.

Sirsat, S.K., Sonar, M.A., Wanjarwadkar, K.M. and Kadam, V.B., 2023. Study of the aquifer vulnerability by longitudinal unit conductance, GOD and GLSI Models in the Painganga river basin, Buldhana (Maharashtra, India). *Journal of Indian Geophysical Union*, *27*(4), pp.281-291.

Srinivasa Gowd, S., 2004. Electrical resistivity surveys to delineate groundwater potential aquifers in Peddavanka watershed, Anantapur District, Andhra Pradesh, India. *Environmental Geology*, *46*, pp.118-131. https://doi.org-/10.1007/s00254-004-1023-2.

Suneetha, N. and Gupta, G., 2018. Evaluation of groundwater potential and saline water intrusion using secondary geophysical parameters: A case study from western Maharashtra, India. In: E3S web of Conferences, Vol. 54. EDP Sciences, p. 00033. https://doi.org/10.1051/e3sconf/20-185400033.

Stacher, P., 1995. Present understanding of the Niger Delta hydrocarbon habitat. In: Geology of Deltas. pp. 257 – 267. A.A. Balkema, Rotterdam, Netherlands.

Stempvoort, D.V., Ewert, L. and Wassenaar, L., 1993. Aquifer vulnerability index: a GIS-compatible method for groundwater vulnerability mapping. *Canadian Water Resources Journal*, 18(1), pp.25-37. https://-doi.org/10.4296/cwrj1801025.

Thomas, J.E., George, N.J., Ekanem, A.M. and Nsikak, E.E., 2020. Electrostratigraphy and hydrogeochemistry of hyporheic zone and

water-bearing caches in the littoral shorefront of Akwa Ibom State University, Southern Nigeria. *Environmental Monitoring and Assessment*, *192*, pp.1-19. https://doi.org/10.1007/s10661-020-08436-6.

Udosen, N.I. and George, N.J., 2018a. A finite integration forward solver and a domain search reconstruction solver for electrical resistivity tomography (ERT). *Modeling Earth Systems and Environment*, 4, pp.1-12. https://doi.org/10.1007/s40808-018-0412-6.

Udosen, N.I. and George, N.J., 2018b. Characterization of electrical anisotropy in North Yorkshire, England using square arrays and electrical resistivity tomography. *Geomechanics and Geophysics for Geo-Energy and Geo-Resources*, 4, pp.215-233. https://doi.org/10.1007/s40948-018-0087-5.

Udosen, N. and Potthast, R., 2018. Automated optimization of electrode locations for electrical resistivity tomography. *Modeling Earth Systems and Environment*, 4, pp.1059-1083. https://doi.org/10.1007/s40-808-018-0472-7.

Udosen, N. and Potthast, R., 2019. A framework for solving meta inverse problems: experimental design and application to an acoustic source problem. *Modeling Earth Systems and Environment*, 5, pp.519-532. https://doi.org/10.1007/s40808-018-0541-y.

Udosen, N.I., 2022. Geo-electrical modeling of leachate contamination at a major waste disposal site in south-eastern Nigeria. *Modeling Earth Systems and Environment*, 8(1), pp.847-856. https://doi.org/10.1007/-s40808-021-01120-9.

Udosen, N.I., Ekanem, A.M. and Thomas, J.E., 2023. Evaluation and modeling of a major coastal aquifer's vulnerability to contamination with the use of GOD and AVI models as indicators in South - eastern Nigeria. *Researchers Journal of Science and Technology*, 3(4), pp.61-78.

Udosen, N.I., Ekanem, A.M. and Thomas, J.E., 2024a. Geo-hydraulic characterization of a coastal aquifer system in South-eastern Nigeria with the inverse slope method. *Researchers Journal of Science and Technology*, 4(1), pp.1-20.

Udosen, N.I., Ekanem, A.M. and George, N.J., 2024b. Modeling of aquifer geo-hydraulic characteristics with geo-electrical methods at a major coastal aquifer system in Uyo, southern Nigeria. *Water Practice & Technology*, 19(2), pp.611-628. https://doi.-org/10.2166/wpt.2024.018.

Udosen, N.I., Ekanem, A.M. and George, N.J., 2024c. Geophysical exploration to assess leachate percolation and aquifer protectivity within hydrogeological units at a major open dump in Eket, Nigeria. *Results in Earth Sciences*, p.100022. https://doi.org/10.1016-/j.rines.2024.100022.

Udosen, N.I., Ekanem, A. M., George, N.J. and Thomas, J. E., 2024d. Geoelectrostratigraphic assessment of aquifer potential, protectivity, and pliable level of vulnerability within a coastal milieu. *Water Practice & Technology*, *19*(5), 2010-2031. https://doi.org/10.2166/wpt.2024.125.

Udosen, N.I., Ekanem, A.M. and George, N.J., 2024e. Geo-electrical prognosis of aquifer protectivity, corrosivity, and vulnerability via index-based models within a major coastal milieu. *Discover Geoscience*, *2*(1), p.18. https://doi.org/10.1007/s4428802400-020-6.

Udosen, N.I., Ekanem, A.M. and George, N.J., 2024f. Litho-stratigraphic characterization of hydrogeological and hydraulic flow units via electrical resistivity, Stratigraphic Modified Lorenz Plots, and flow zone indicator models. *Solid Earth Sciences*, *9*(3), p.100191. https://doi.org/10.1016/j.sesci.2024.100191

Udosen, N.I. and George, N.J., 2024g. Evaluation of specific retention, specific yield, and storage-dependent drainability efficiency in a coastal milieu via geo-electrical technology. *Water Practice & Technology*, p.wpt2024208. https://doi:10.2166/wpt.2024.208.

Udosen, N.I., Ekanem, A.M. and George, N.J., 2024h. Appraisal of flood-prone litho-stratigraphic units via geo-electrical technology. *Malaysian Journal of Geosciences*, 8(1), pp.33-44. https://doi.org/10.26480/mjg.01.2024.33.44.

Udosen, N.I., George, N.J. and Ekanem, A.M., 2024i. Aquifer vulnerability valorization via DRASTIC index-based assessment within litho-facies of a coastal environment. *Results in Earth Sciences*, 2, p.100033. https://doi.org/10.1016/j.rines.2024.100033

Udosen, N.I., Potthast, R.W.E. and Astin, T.R., 2011, Novel framework for finding optimal measurement locations. In 73rd EAGE Conference and Exhibition incorporating SPE EUROPEC 2011 (pp. cp-238). European Association of Geoscientists & Engineers, May 2011, Vienna, Austria. https://doi.org/10.3997/2214-4609.20149569.

Udosen, N.I., Potthast, R.W.E. and Astin, T.R., 2013a. A domain search reconstruction algorithm for electrical resistivity tomography. In 75th EAGE Conference & Exhibition incorporating SPE EUROPEC 2013 (pp. cp-348). European Association of Geoscientists & Engineers, June 2013, London, United Kingdom. https://doi.org-/10.3997/22144609.20130960.

Udosen, N.I., Potthast, R.W.E. and Astin, T.R., 2013b. Automated optimisation of electrode locations to image 2D resistivity anomalies. In 75th EAGE Conference & Exhibition incorporating SPE EUROPEC 2013 (pp. cp-348). European Association of Geoscientists & Engineers, June 2013, London, United Kingdom. https://doi.org/10.3997/2214460-9.20130966.

Ugada, U., Ibe, K. K., Akaolisa, C. Z. and Opara, A. I., 2014. Hydrogeophysical evaluation of aquifer hydraulic characteristics using surface geophysical data: A case study of Umuahia and environs, Southeastern Nigeria. *Arabian Journal of Geosciences*, 7, 5397–5408. https://doi.org/10.1007/s1251-7-013-1150-8.

Vander Velpen, B.P.A., 1988. Resist, a computer program for the interpretation of resistivity sounding curve. An ITC. M. Sc. Research Project. ITCD, Delft, The Netherlands.

Vander Velpen, B.P.A., Sporry, R.J., 1993. RESIST. A computer program to process resistivity sounding data on pc compatibles. *Computer Geosciences*. 19 (5), 691–703. https://doi.org/10.1016/0098-3004(93)90102-b.

Vijayaprabhu, S., Aravindan, S., Kalaivanan, K., Venkatesan, S. and Ravi, R., 2024. Groundwater investigation through vertical electrical sounding: a case study from southwest Neyveli Basin, Tamil Nadu. *International Journal of Energy and*

Water Resources, *8*(1), pp.17-34. https://-doi.org/10.1007/s42108-022-00182-4.

Warsi, T., Kumar, V.S., Dhakate, R., Manikyamba, C., Rao, T.V. and Rangarajan, R., 2019. An integrated study of electrical resistivity tomography and infiltration method in deciphering the characteristics and potentiality of unsaturated zone in crystalline rock. *HydroResearch*, 2, pp.109-118. https://doi.org/10.1016/j.hydres.2019-.11.009.

Yadav, G. S. and Abolfazli, H., 1998. Geoelectrical soundings and their relationship to hydraulic parameters in semiarid regions of Jalore, northwestern India. *Journal of Applied Geophysics*, 39(1), 35–51. https://doi.org/10.1016/s09269851-(98)00003-2.

Zaini, M.S.I. and Hasan, M., 2024. Application of Electrical Resistivity Tomography in Landfill Leachate Detection Assessment. In *A Review of Landfill Leachate: Characterization Leachate Environment Impacts and Sustainable Treatment Methods* (pp. 1-22). Cham: Springer Nature Switzerland. https://doi.org/10.1007/9783-031-55513-8_1.

Zhdanov, M.S., 2002. *Geophysical inverse theory and regularization problems* (Vol. 36). Elsevier. Amsterdam.

Zohdy, A.A., Eaton, G.P. and Mabey, D.R., 1974. Application of surface geophysics to groundwater investigations. USGS Techniques of water resources investigations, Book 2. https://doi.org/10.3133/twri0-2d1.